

Sustained-release profenofos encapsulated polylactic acid nanofibres: Evaluation in maize cultivation under actual field conditions

Liem Thanh Nguyen^{1*} , Vu Anh Doan¹ , Tuan Anh Phung¹ 

¹ School of Materials Science and Engineering, Hanoi University of Science and Technology, Hanoi Vietnam

* Corresponding author e-mail: liem.nguyenthanh@hust.edu.vn

ABSTRACT

This study investigated the impact of nano pesticide formulations based on profenofos/polylactic acid nanofibre scaffolds. Using the coaxial electrospinning approach, nanofibers were obtained with an average diameter of 495.74 ± 86.46 nm. The release profile analysis revealed that approximately 32.6% of the active ingredient was released within the initial two weeks, increasing to around 82.15% after 15 weeks. The release pattern followed a non-Fickian behaviour, likely governed by both diffusion and swelling of the polylactic acid matrix. In field applications on maize, two scaffold-based formulations demonstrated prolonged protective effects, maintaining efficacy levels of 89.24–93.35%, compared with only 11.9% for the commercial pesticide Selecron 500EC after two weeks. These results demonstrate improved pest control performance of profenofos/polylactic acid nanofibre scaffolds. However, the experiment was based on an unreplicated field trial and did not include residue analysis, which limits the strength of the environmental interpretation. Therefore, the findings should be viewed as preliminary, and further studies are needed before drawing definitive conclusions about environmental benefits.

Keywords: coaxial electrospinning, nanofibre, pesticide, profenofos, slow release.

INTRODUCTION

Plant diseases are estimated to cause around 16% of global crop yield losses, posing a significant threat to food security. To address pest infestations and sustain agricultural productivity, a wide range of pesticide products has been used worldwide. However, in developing countries, such as Vietnam, the habitual and intensive use of pesticides raises concerns about adverse effects on soil, water, and non-target ecosystems. This highlights a critical challenge for agriculture: enhancing crop yields while promoting the rational and environmentally sustainable application of pesticides (Oerke, 2006; Ficke et al., 2018; Eash et al., 2019; Akhtar et al., 2024).

The global market for crop protection chemicals in 2024 is projected to reach USD 64.18 billion (Crop Protection Chemicals Market

Size, 2025). While pesticides play a crucial role in safeguarding crop yields, their frequent and intensive application has raised growing concerns regarding environmental persistence and toxicological risks to both ecosystems and human health (Leskovac et al., 2023; Schneider et al., 2023). Overuse and large-scale deployment of these chemicals have been linked to reduced soil biodiversity and detrimental effects on terrestrial as well as aquatic environments. In addition, pesticide misuse has contributed to surface water and groundwater contamination through toxic runoff, further amplifying ecological risks (Khatri et al., 2015; Jayaraj et al., 2016; Wagh et al., 2020; Ristaino et al., 2021).

Excessive pesticide application has had detrimental consequences for the environment, ecosystems, and human health, thereby threatening the long-term sustainability of agricultural

practices. This situation underscores the urgent need to reassess the current pesticide use. To mitigate such impacts, researchers have emphasised the importance of developing innovative technologies, implementing mitigation measures, and adopting more efficient application strategies in the field (Chen et al., 2020; Sur et al., 2022; Jain et al., 2024; Zhou et al., 2025). Recently, nano-formulated pesticides have emerged as a promising alternative in agriculture, offering several advantages over conventional products. These include improved solubility, controlled release that enhances pesticide efficiency, protection of active compounds from premature degradation, and a notable reduction in offensive odours during handling and application (Ahlawat et al., 2021; An et al., 2022)

Nano-based pesticides are generally defined as nanoscale particles, materials incorporating active pesticide ingredients, or other nano-structured entities with pesticidal potential. Research has demonstrated that such formulations can enhance the dispersion and wettability of agricultural products. Moreover, nanomaterials and biodegradable carriers possess desirable properties, such as mechanical strength, permeability, and biodegradability that make them suitable for developing advanced nano-pesticide systems (Yousef et al., 2023).

Yu et al. (2007) investigated nano TiO₂ membranes for photocatalytic degradation of organochlorine pesticides, reporting that the adsorption of peroxides or hydroxyl radicals, coupled with electron transfer processes, accelerated the breakdown of pesticides on the TiO₂ surface.

In 2016, Roshani and colleagues reported the sustained release of thiram from poly (L-lactic acid) nanofibre mats, demonstrating that such systems could provide effective long-term and controlled pesticide delivery for agricultural use (Roshani et al., 2016). Ethyl formate, a naturally occurring volatile compound with both insecticidal and antimicrobial activity, has also been explored as an alternative to synthetic fumigants. Its controlled release delayed microbial growth on strawberries for up to 10 days at 5°C, highlighting potential applications in active food packaging (Zaitoon et al., 2021). Further evidence from Wang's research confirmed that nano-formulated pesticides generally exhibit greater efficacy against target pests than conventional formulations, largely because premature losses of active ingredients are minimised (Wang et al., 2022).

Over the last two decades, electrospinning has become a versatile and innovative technique for producing nano materials. This method has been increasingly adopted in nano-pesticide research, leading to advances, such as embedding essential oils into PLA-based nanocarriers, employing green synthesis routes for neem extract and neem oil-derived Azadirachtin, and evaluating their pesticidal effectiveness against Fall Armyworm (Zaitoon et al., 2021; Audelo et al., 2022; Modaf-feri et al., 2024).

Profenofos (O-(4-bromo-2-chlorophenyl) O-ethyl S-propyl phosphorothioate) has been extensively utilised as a pesticide since 1965 and remains widely applied in agriculture, particularly in developing countries (Sun et al., 2025). It is effective against a broad spectrum of pests, including brown planthoppers, green leafhoppers, leaf rollers, and armyworms. In Vietnam's tropical conditions characterised by high temperatures, humidity, and strong sunlight the residual effectiveness of conventional pesticides diminishes rapidly. As a result, farmers often resort to repeated applications, sometimes exceeding recommended or legal limits. Such practices contribute to environmental contamination and elevate the risk of pesticide residues in food products. To address these issues, there is increasing interest in innovative pesticide delivery systems with slow-release properties that maintain efficacy over time, reduce application frequency, and support environmentally sustainable agriculture.

The present study explored the biological performance of profenofos/poly(lactic acid) (PFF/PLA) core/shell nanofibres fabricated through electrospinning, prepared in both suspension concentrate (SC) and wettable powder (WP) formulations. Their effectiveness against *Spodoptera frugiperda* in maize was assessed, alongside their influence on crop growth and development, thereby contributing to sustainable pest management strategies.

MATERIAL AND METHODS

Materials

Poly(lactic acid) (PLA, Resomer® R203H, Mw 18,000–24,000, density 1.24 g/cm³, Tg 48–52 °C) was obtained from Sigma-Aldrich. Chloroform (≥ 99%) and N,N-dimethylformamide (≥ 99.5%) were supplied by Xilong Scientific Co.,

Ltd. (China). Profenofos (95%, density 1.41 g/cm³) was purchased from DC Chemical Co., Ltd. (China). For comparison, Selecron 500 EC (containing 500 g/L profenofos) was provided by Syngenta Co., Ltd. (Vietnam) and used as a reference pesticide formulation.

Additional reagents included tristyrilphenol ethoxylates (viscosity 920 cps), alkyl naphthalene sulfonate (39.2%, unsulphonated oil content < 1.25%), nano-silica (99.7%, particle size ~200 nm), sodium lignosulfonate (density 0.5 g/cm³), lauryl sodium sulphate (Tm 206 °C, water soluble), emulsifying agent Vanzan NF (viscosity 1400-1600 mPa·s, particle size ~180 µm), and kaolin, all sourced from Xilong Scientific Co., Ltd. (China). All chemicals were utilized without further purification.

Preparation of PFF/PLA nanofibre scaffolds

Electrospinning was carried out using a shell solution with a concentration of 8 wt.%, at a feed rate of 0.6 mL/h, while the core solution was supplied at 0.18 mL/h. The distance between the needle tip and the collector was maintained at 16 cm, under an applied voltage of 16 kV. All experiments were conducted under ambient conditions of 25 ± 2°C and 50% relative humidity. A schematic illustration of the coaxial electrospinning apparatus is presented in Figure 1.

For the shell solution, PLA was dissolved in a chloroform/N,N-dimethylformamide mixture (75:25, w/w). An 8.0 wt.% PLA solution was prepared by magnetic stirring at 50-55 °C for one hour to achieve complete dissolution.

The core solution, consisting of 95% profenofos (PFF), was loaded into a 5 mL syringe equipped with a steel needle. Core/shell nanofibres were fabricated using a coaxial spinneret. The

inner needle (30G) had inner and outer diameters of 0.16 mm and 0.31 mm, respectively, while the outer needle (21G) had corresponding diameters of 0.51 mm (inner) and 0.82 mm (outer).

Characterisation of PFF/PLA scaffolds

PFF/PLA nanofibre diameter measurements were performed using a scanning electron microscope (SEM-JSM-6510LV, JEOL, Japan). Prior to imaging, the nanofiber samples were coated with a thin gold layer to improve surface conductivity. Images were captured at a magnification of 5000×, and fibre diameters were determined using ImageJ software. Measurements were taken from at least five representative fields to obtain the average fibre diameter and its distribution.

To determine the fibre diameter: after the spinning process becomes stable (about 5 minutes), a glass slide is used to collect fibres on the surface. For statistical reliability, about 40 – 50 fibres were randomly selected from the SEM images to determine average diameter and distribution. This procedure is repeated 3 times during spinning to ensure the results are representative.

The core-shell morphology of FFF/PLA nanofibers was examined using a transmission electron microscope (TEM - JEM-2100, Jeol, Japan) operated at 200 kV PFF/PLA nanofibre samples were prepared by electrospinning PFF/PLA solutions directly onto carbon-coated copper grids for about 5 seconds. The grids were then observed under the TEM to obtain high resolution images of the core-shell structure. Because the electron beam must penetrate the entire fibre cross section, only fibres with diameters below 300 nm were selected to ensure clear visualisation of the internal structure.

Chemical structure analysis was carried out using attenuated total reflectance Fourier-transform

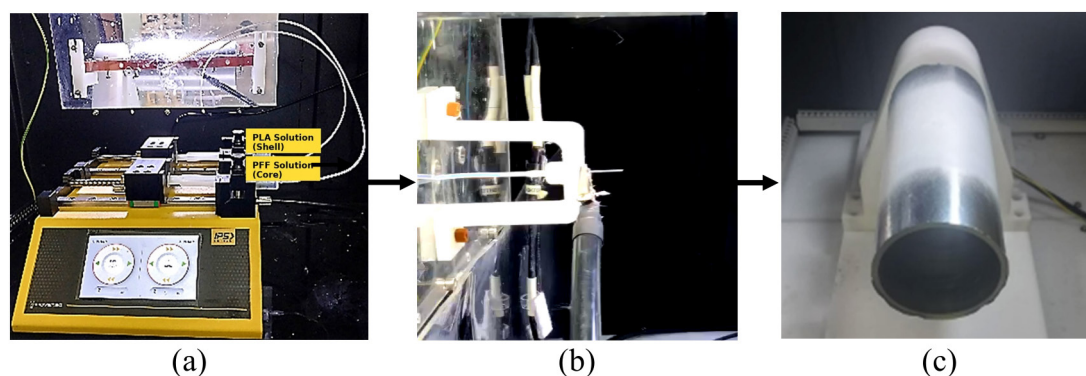


Figure 1. Schematic view of coaxial electrospinning process: syringe pump (a), coaxial spinneret (b), collector (c)

infrared spectroscopy (ATR-FTIR, Nicolet iS20). Spectra of pure profenofos and PFF/PLA nanofiber scaffolds were collected in the range of 4000–500 cm⁻¹, with 64 scans at a resolution of 4 cm⁻¹.

The profenofos content in the nanofibres, or the PFF released at the time, was quantified by gas chromatography (GC-6890N Agilent, USA). The PFF concentration was determined by gas chromatography with a flame ionisation detector (FID). Triphenyl phosphate was used as the internal standard. Approximately 10 g of PFF/PLA nanofiber scaffolds were randomly collected and dissolved in 10 mL of n-hexane using an ultrasonic bath until complete homogenisation was achieved. An HP-5 nonpolar capillary column was used for GC-FID analysis. The detector (FID) temperature at 280 °C and the injector temperature was set at 250 °C.

Release behaviour studies

For loading capacity determination, approximately 10 g of PFF/PLA nanofiber scaffolds were randomly collected and dissolved in 10 mL of n-hexane using an ultrasonic bath until complete homogenisation was achieved. The resulting solutions were analysed by GC to quantify the amount of PFF incorporated within the PFF/PLA nanofiber scaffold. The loading capacity of PFF in the nanofibers was then calculated (Equation 1).

$$\frac{\text{The total PFF content encapsulated in fibres}}{\text{The initial weight of the tested sample}} \times 100 \quad (1)$$

The in vitro release profile of PFF/PLA nanofibres was assessed by immersing scaffold samples (10 g, cut into squares) in 40 mL of deionised water maintained at 28°C - 40°C for up to 84 days. At intervals of five days, from week 1 through week 15, aliquots were collected for HPLC analysis to determine the amount of profenofos released. The cumulative release of PFF at each time point was calculated, and the release kinetics were expressed as a function of time (Equation 2). The release of PFF was tested three times using three different PFF/PLA scaffolds, and the average value was reported.

$$\text{Release (\%)} = \frac{M_t}{M_\infty} \times 100 \quad (2)$$

where: M_t – the amount of PFF released at time t , M_∞ – is the total amount of PFF in the scaffold.

The study of release kinetics provides essential information on the behaviour and efficiency

of drug delivery systems. To better understand the transport mechanisms and correlate them with material properties, the Korsmeyer-Peppas model is commonly applied. In this model, the release rate constant (k) and the diffusion exponent (n), known as the Korsmeyer-Peppas coefficient, are derived from the ratio of the cumulative amount of PFF released at a given time (M_t) to the total amount of PFF in the scaffold (M_∞) (Equation 3).

$$f = \frac{M_t}{M_\infty} = kt^n \quad (3)$$

where: M_t – the amount of PFF released at time t , M_∞ – total amount of PFF in the scaffold, k – the kinetic constant characteristic of the material system, n – the diffusion exponent indicating the release mechanism.

Preparation of the nano-pesticide products from PFF/PLA nanofiber scaffold

Two nano-formulated pesticide types were developed based on a nanofibrous scaffold consisting of PFF as the core and PLA as the shell, serving as the carrier matrix for encapsulating the active ingredient. The formulations were designed in accordance with the Vietnam National Standard TCVN 12561:2022 (*Pesticides – Bio efficacy Field Trials*), which aligns with FAO/WHO guidelines for pesticide preparation and evaluation. Each formulation was produced with specific ratios of raw materials, including the active pesticide encapsulated within the PFF/PLA scaffold (Table 1).

For the suspension concentrate (SC) nano-pesticide formulation, PFF/PLA nanofibres and sodium lignosulfonate (dispersing agent) were

Table 1. Formulation composition for nano pesticides (SC, WP)

Components	Weight ratio, %	
	SC	WP
PFF/PLA nanofiber scaffolds	30	30
Tristyrylphenol ethoxylates	-	4
Alkyl naphthalene sulfonate	-	4
Nano silica	-	3
Kaolin	-	59
Sodium lignosulfonate	5	-
Lauryl sodium sulfate	4	-
Vanzan NF	5	-
Water	56	-
Total	100	100

dispersed in water within a reactor and pre-mixed at 600 rpm to form an initial suspension. Sodium lauryl sulphate as surfactant was then incorporated, and the mixture was stirred at 1000 rpm for 60 min. The dispersion was subsequently ground to obtain the required particle size, after which suspending agent Vanzan NF was introduced. Final homogenisation was performed for 2 h at approximately 1000 rpm.

For the wettable powder (WP) nano-pesticide formulation, tristylphenol ethoxylates as dispersing agent, alkyl naphthalene sulfonate as surfactant, and anti-caking agent nano-silica were initially combined in a mechanical mixer for 5 min. PFF/PLA nanofibres were then added, and mixing was continued for an additional 15 min. The resulting mixture was processed in a disc mill at 1500 rpm for 60 min to achieve a particle size

smaller than 10 μm . The synthesised pesticide in the laboratory and Selecron 500 EC (Fig. 2).

Field trial under actual field conditions

The field experiment block design and test location are shown in Figure 3. A small-scale field trial was carried out in Le Chi Commune, Gia Lam District, Hanoi, Vietnam, from 18th March to 1st May 2025. The test crop was hybrid maize (F1-HN45) at the vegetative stage (5–6 leaves). The planting process started with seed sowing on March 18th, 2025. When the plants reached the 5–6 leaf stage, pesticide spraying was carried out (on April 18, 2025). The pesticide was applied only once, followed by an evaluation of pest development over 14 days, which concluded on May 1st, 2025.

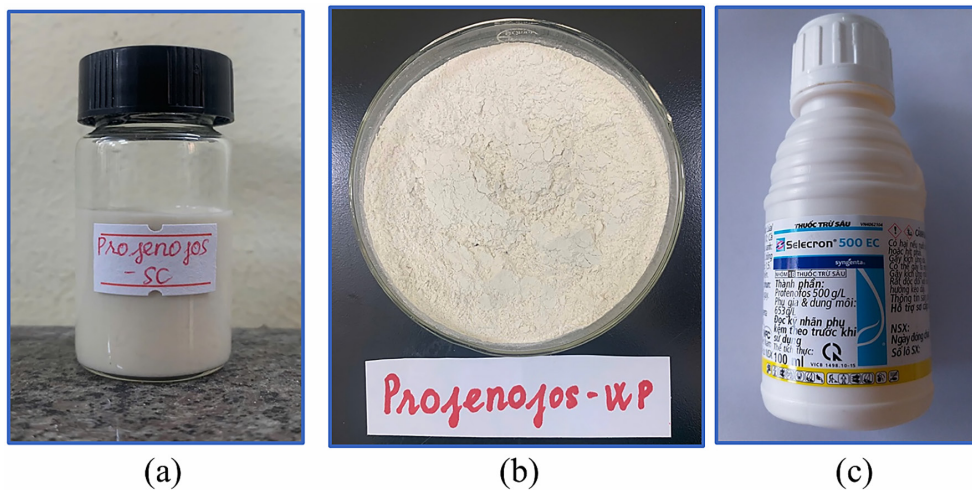


Figure 2. Digital images of nano PFF/PLA pesticides: SC (a), WP (b), Selecron 500EC (c)

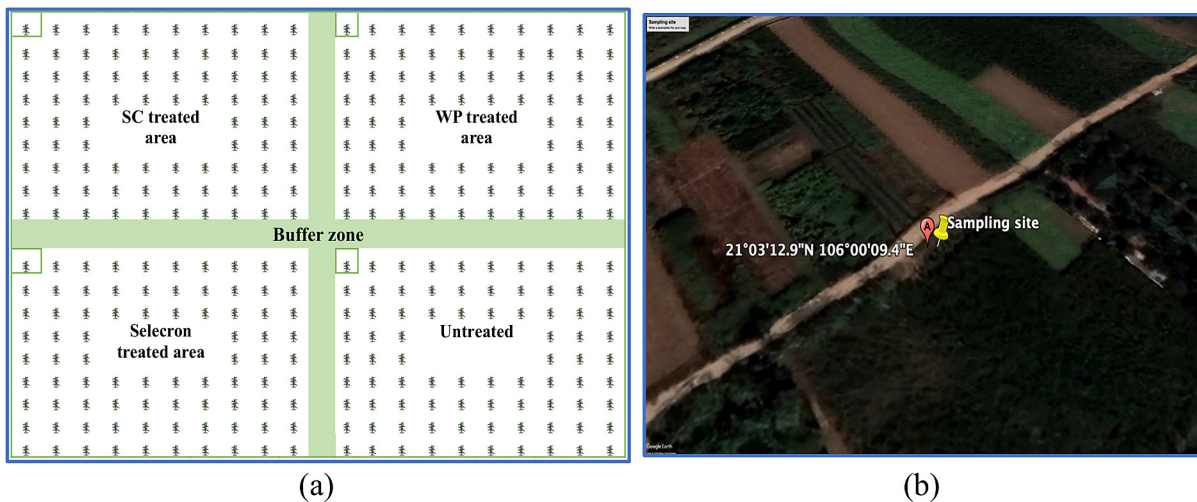


Figure 3. Field experiment block design (a), test location at Le chi, Hanoi (b)

Each experimental plot measured 360 m² and was arranged sequentially without replication. To minimise external interference, a 1.0 m buffer zone separated adjacent plots, and the entire test area was positioned at least 1.0 m from the field boundaries.

The site was located at 21.03129° N, 106.0009° E, with an elevation of 6 m above sea level. The soil at the site was classified as light loam. For each 360 m² plot, fertilisation included 500 kg of manure, 25 kg of superphosphate, 10 kg of urea, and 8 kg of potassium chloride. The field was managed under a rotation system with other short-duration crops. During the trial, weather conditions were favourable: on the day of pesticide application, temperatures ranged between 23–29 °C with sunny skies and light winds, while the following days remained mostly sunny. The target pest for the field trial was the early instar larvae (1st – 2nd instars) of the fall armyworm (*Spodoptera frugiperda*), which were actively emerging and infesting the maize crop with a steadily increasing population density. No additional harmful organisms were detected in the experimental plots. The effectiveness of the pesticide treatments against fall armyworm infestation was assessed using the Henderson-Tilton formula, which calculates efficacy based on larval population density recorded during each survey (Equation 4).

$$E (\%) = 1 - \frac{T_a \cdot C_b}{T_b \cdot C_a} \times 100 \quad (4)$$

where: E – effectiveness of the tested pesticide, (%), T_a , T_b – density of live fall armyworms in the treated plot after, before treatment, C_a , C_b – density of live fall armyworms in the control plot after, before treatment

RESULTS AND DISCUSSION

Characterisation of PFF/PLA scaffolds

PFF/PLA scaffolds were fabricated under the conditions described earlier, and their FTIR absorption spectra, along with that of neat profenofos, are presented in Figure 4. In the spectrum of the PFF/PLA nanofibres, only the characteristic absorption peaks of PLA were detected, including the prominent ester carbonyl band at 1745 cm⁻¹ and the C - O - C stretching vibrations at 1179.7 and 1080 cm⁻¹. In contrast, the distinctive absorption bands of profenofos such as P=O stretching (1226 cm⁻¹), C - O - C and P - O - C stretching (1018 cm⁻¹), aromatic C - H out-of-plane vibration (914 cm⁻¹), and aliphatic C - H stretching/bending (2957 and 1472 cm⁻¹) were not observed in the composite spectrum. This absence indicates that profenofos was not present on the fibre surface but was successfully encapsulated within the PLA matrix.

The morphological features and diameter distribution of the nanofibers obtained under the

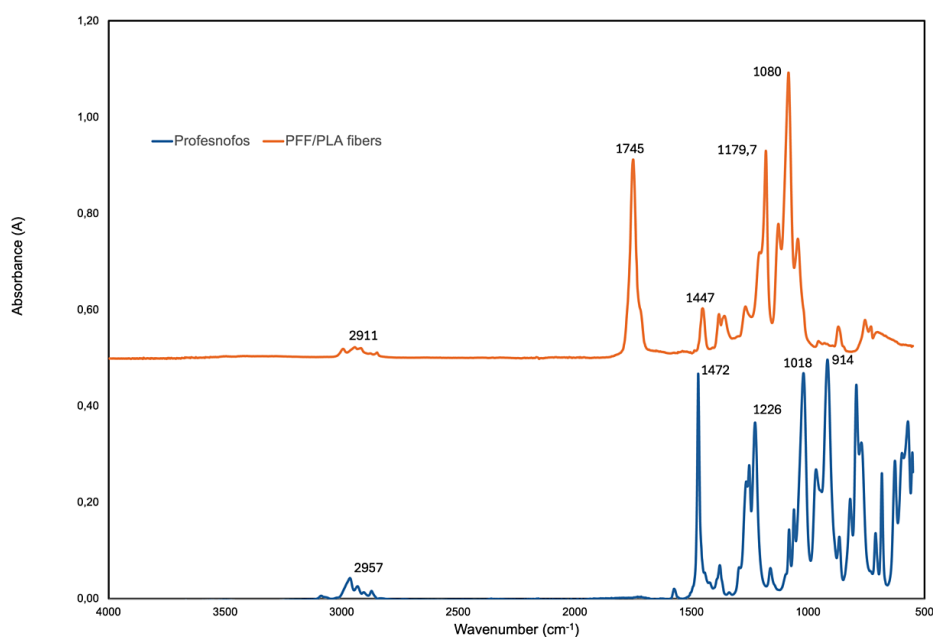


Figure 4. FTIR spectra of profenofos and PFF/PLA nanofibres

optimized fabrication conditions are shown in Figure 5. Surface inspection of the PFF/PLA nanofibers by SEM method revealed no observable voids and the fibres exhibited a uniform morphology, with an average diameter of 495.74 ± 86.46 nm. These findings are consistent with the FTIR results, which indicated the absence of profenofos specific peaks on the fibre surface, further suggesting that the active ingredient was encapsulated within the PLA matrix rather than exposed externally.

Figure 6 shows that the PFF content in the fibres varies significantly depending on the PFF concentration in the core of the PFF/PLA nanofibres. The total amount of PFF in the nanofibre mat was determined by GC analysis and

calculated using Equation (1). Under the electrospinning conditions described in section 2.2, the PFF loading in the PFF/PLA nanofibres reached up to 76.834%. Under the fabrication conditions (solution concentration and core/shell feed rate), the theoretical PFF content was expected to reach 78.082%. However, GC analysis showed that the actual PFF content in the PFF/PLA nanofibres was 76.834%, corresponding to an encapsulation efficiency of 98.4%. This slight difference can be explained by the loss of a small amount of PFF that was likely carried away with the solvent during the electrospinning process.

Slow-release pesticide formulations represent an important advancement in pest management,

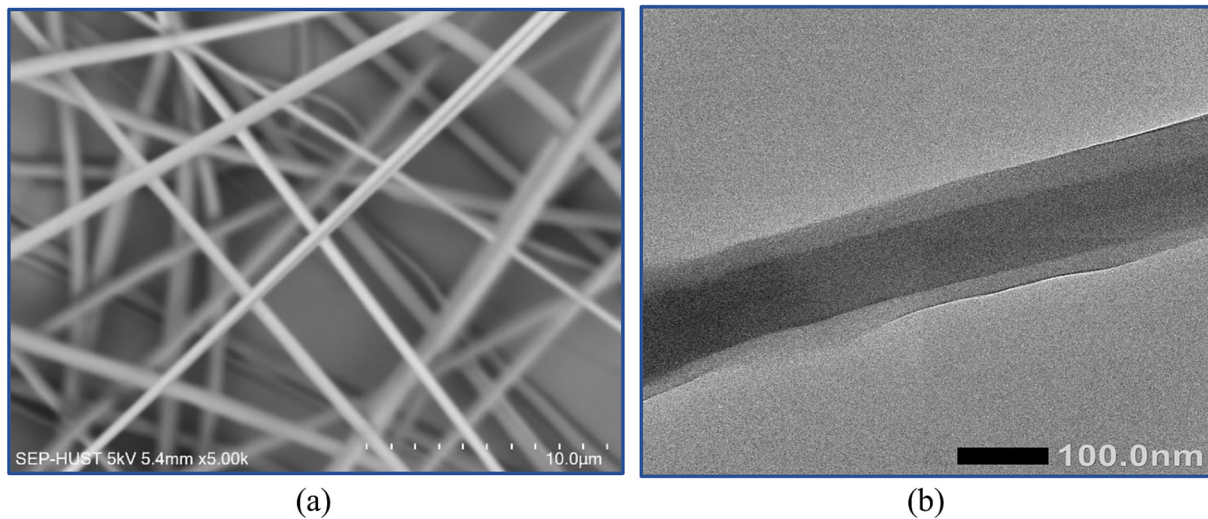


Figure 5. SEM image (a) and TEM image (b) of PFF/PLA nanofibres

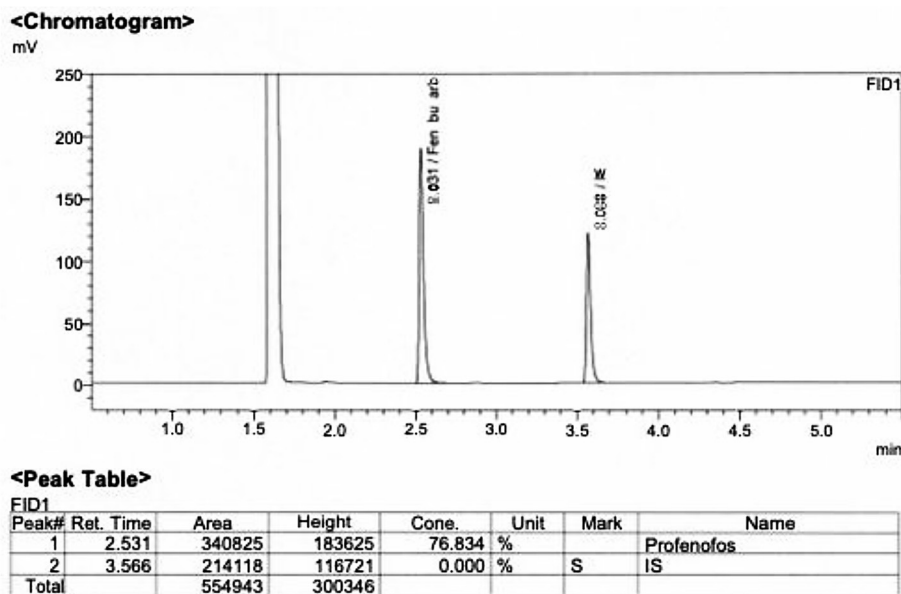


Figure 6. PFF loading content

integrating nanotechnology with controlled-release systems. By encapsulating active ingredients, these formulations enable a gradual and sustained release, thereby reducing the frequency of applications, lowering labour costs, and improving field efficiency. Such systems are also vital for minimising environmental risks while maintaining efficacy. According to Vietnamese guidelines, a slow-release formulation should demonstrate controlled release for at least 21 days under standardised conditions at 25°C.

In this study, the release behaviour of profenofos from PFF/PLA nanofiber scaffolds was evaluated, and the corresponding kinetic model was determined (Fig. 7). The cumulative release profile was monitored over a 15 weeks period, with the released amount calculated according to Eq. 2. To further elucidate the release mechanism and establish the structure function relationship of the core - shell scaffolds, the Korsmeyer Peppas kinetic model was applied (Equation. 3).

As it was shown in Figure 7a, approximately 32.6% of the total profenofos content was released during the first two weeks. By week 15, cumulative release reached about 82.15%. The release kinetics displayed a biphasic trend, consisting of an initial rapid release of loosely bound profenofos located on the scaffold surface, followed by a sustained and gradual release from within the nanofiber matrix. This dual-phase behaviour highlights both the structural integrity and the controlled-release capability of the PFF/PLA formulation.

To further clarify the release mechanism, a kinetic study was performed to analyse the release

profile, providing insight into the functional performance of the fibrous delivery system. As it was illustrated in Figure 7b, the calculated release exponent (n) was 0.5842, which falls within the range of $0.43 < n < 0.85$. This indicates that the release of profenofos from the PFF/PLA membranes follows a non-Fickian transport model. Such behaviour suggests that the release process is jointly governed by Fickian diffusion and polymer relaxation or swelling, involving both the pesticide encapsulated in the core and the PLA shell matrix. The results of the release kinetics also indicate that fabricating PFF loaded microfibrils using PLA or other biodegradable polymers could be effective for real agricultural applications. The release of active substances requires polymer swelling in water and a moisture gradient between the fibre and the surrounding environment. Irrigation may introduce water into the microfibrils but may also wash away fibres from plant stems or leaves. The use of polymers with strong adhesion to plant surfaces or with superabsorbent properties should therefore be considered and further developed.

SEM analysis demonstrated that after two weeks of immersion, the surface of the PFF/PLA nanofibres showed clear signs of degradation, characterised by the formation of multiple pores, while the overall circular morphology of the fibres was still largely maintained. These morphological changes are attributed to the gradual release of profenofos during immersion and the partial degradation of the PLA shell, consistent with its biodegradable nature. After 15 weeks of immersion, the nanofibre morphology exhibited pronounced

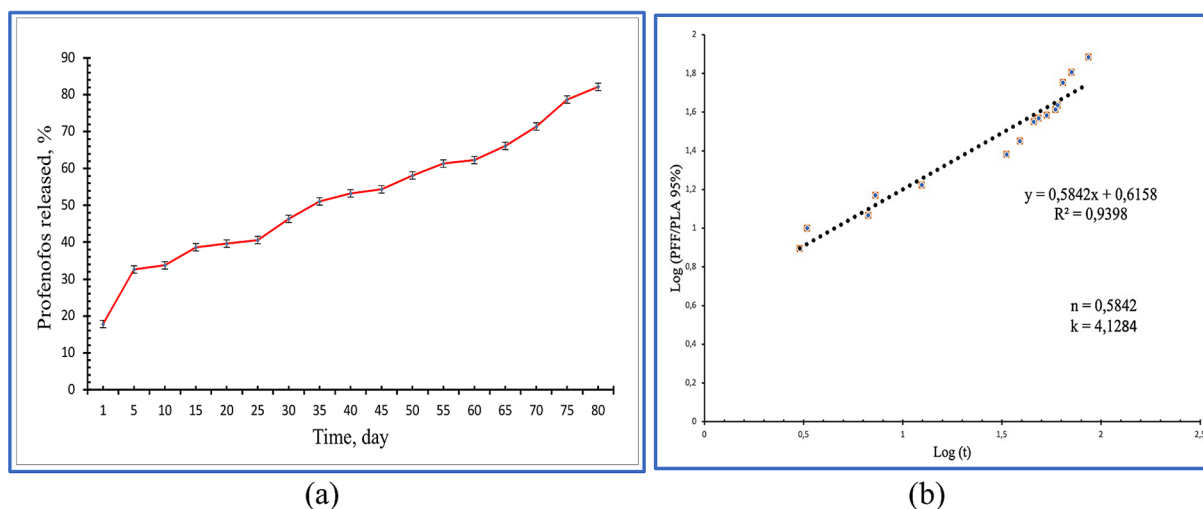


Figure 7. PFF release rate (a), Release profile curve (b)

alterations. The originally distinct, circular fibres became flattened, and many fibres adhered to one another. This structural collapse and aggregation may account for the plateau observed in the release profile of PFF after 15 weeks. Moreover, the visible outer boundary along the fibres confirmed the presence of a core/shell configuration (Fig. 8).

Field trial under actual field conditions

All pesticide treatments, including both test and control formulations, were applied as a single spray. Each formulation was diluted to achieve a profenofos concentration of 2.5%, in accordance with Vietnam national standards. Application

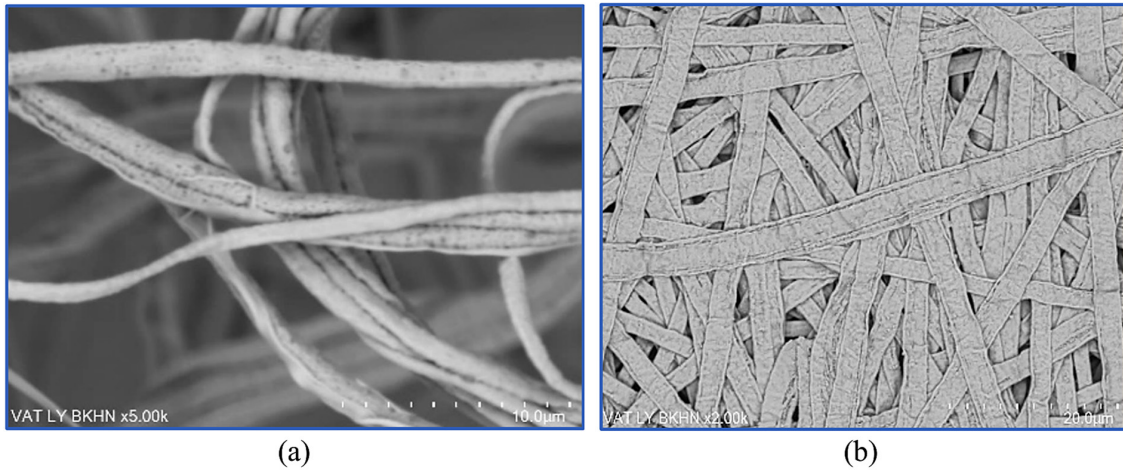


Figure 8. SEM images of PFF/PLA scaffold after 2 weeks of immersion (a), after 15 weeks of immersion (b)

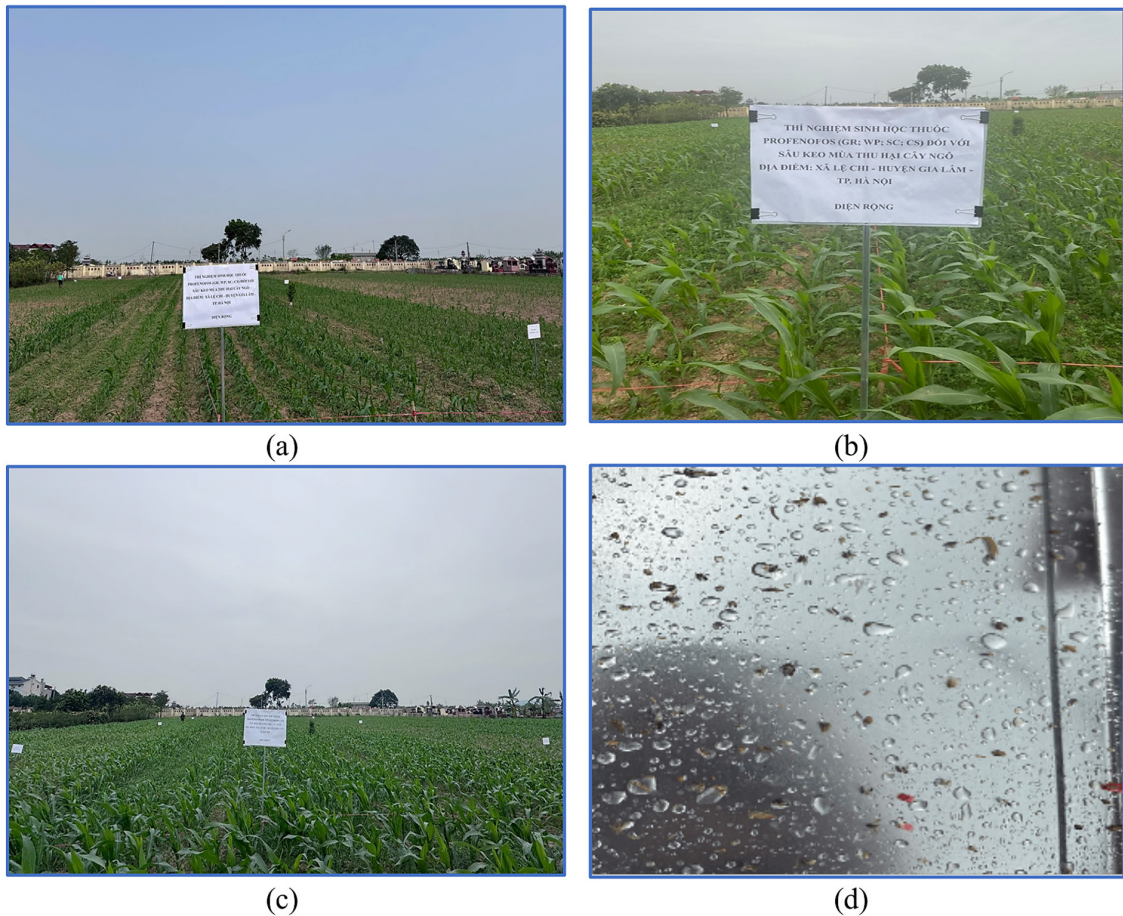


Figure 9. Field trial under actual field conditions: after 1 day of spraying (a), after 5 days of spraying (b), after 14 days of spraying (c), container tray for determining the number of fall armyworm larvae (d)

was carried out when early instar Fall armyworm larvae (1st – 2nd instars) were first detected at a density of 1.04–1.16 larvae per plant. The spraying date was 18th April 2025. For comparison, the commercial formulation Selecron 500 EC, widely used in Vietnam, served as a reference standard. Liquid treatments were applied by thoroughly spraying the maize canopy with 18-liter electric backpack sprayers. To avoid confounding effects, no additional plant protection products were used during the trial.

Efficacy assessments for each treatment were conducted at 10 sampling points arranged along two diagonal transects within the test plot. To minimise border effects, each sampling point was positioned 1 m from the plot edge. At every point, five consecutive fixed plants were examined, and the number of live larvae present was recorded. Pest density was then calculated as the average number of insects per plant. On the basis of the determination of active ingredient content in the SC and WP formulations, and following the TCVN standard requirement of 250 g of active ingredient (profenofos) per hectare, the application dosage for each treatment was established, as summarised in Table 2.

The results of efficacy evaluations for profenofos-loaded PFF/PLA nanofibers, as well as their effects on maize plants at different intervals after treatment, are summarised from tables 3 to table 5. Treatments were applied to maize, and assessments were conducted at 1-, 3-, 5- and 14-days post application. The effects on plant growth and development were evaluated using a

phytotoxicity symptom rating scale: level 1: no visible toxicity; level 2: mild toxicity with slight growth reduction detectable upon close inspection; level 3: clear toxicity symptoms easily visible to the naked eye.

Across all assessment periods, maize plants treated with the suspension concentrate (SC), wettable powder (WP), and the reference formulation Selecron 500 EC exhibited no observable phytotoxicity. This indicates that the tested nano-formulations were safe for maize under the experimental conditions.

To evaluate the efficacy of the insecticide treatments against fall armyworm, periodic field surveys were carried out to record larval survival at different observation intervals. Larval density (insects per plant) was calculated by dividing the number of live fall armyworms observed by the total number of plants examined. The survey outcomes, representing changes in larval population density under each treatment, are shown in Tables 4 and 5.

As summarised in Table 4, both PFF/PLA based formulations demonstrated superior efficacy compared with the conventional profenofos product. At seven days after application, larval densities were recorded as 0.28 larvae/plant for the SC treatment, 0.42 larvae/plant for the WP treatment, and 1.38 larvae/plant for Selecron 500 EC. While SC and WP treatments maintained a gradual reduction in larval density over time, the density in plots treated with Selecron 500 EC increased to 1.38 larvae/plant, exceeding the initial infestation level. This trend indicates a marked

Table 2. Treatment details

Sl. No.	Treatments	Dose		Dilution in water, L/ha
		Technical, g/ha	Formulation, g/ha	
1	SC product	250	1.070.9	500
2	WP product	250	1.070.9	500
3	Selecron 500EC	250	500	500
4	Untreated	0	0	500

Table 3. Effects on maize plants after treatment

Sl. No.	Treatments	Toxicity level						
		1 DAS	3 DAS	5 DAS	7 DAS	10 DAS	12 DAS	14 DAS
1	SC product	1	1	1	1	1	1	1
2	WP product	1	1	1	1	1	1	1
3	Selecron 500EC	1	1	1	1	1	1	1
4	Untreated	1	1	1	1	1	1	1

Note: DAS – days after spray, Untreated – using water only.

Table 4. Density of surviving fall armyworm (*Spodoptera frugiperda*) across survey periods

Sl. No.	Treatments	Density, insects/plant, Mean \pm SD							
		DBS	1 DAS	3 DAS	5 DAS	7 DAS	10 DAS	12 DAS	14 DAS
1	SC product	1.08 \pm 0.09	0.80 \pm 0.03	0.52 \pm 0.03	0.36 \pm 0.02	0.28 \pm 0.01	0.32 \pm 0.01	0.45 \pm 0.02	0.34 \pm 0.01
2	WP product	1.04 \pm 0.08	0.92 \pm 0.02	0.64 \pm 0.04	0.52 \pm 0.03	0.42 \pm 0.02	0.46 \pm 0.02	0.61 \pm 0.03	0.53 \pm 0.02
3	Selecron 500EC	1.16 \pm 0.11	1.00 \pm 0.07	0.76 \pm 0.02	0.54 \pm 0.02	1.38 \pm 0.04	1.94 \pm 0.08	2.16 \pm 0.06	4.84 \pm 0.24
4	Untreated	1.06 \pm 0.09	2.06 \pm 0.24	2.24 \pm 0.29	3.16 \pm 0.22	3.36 \pm 0.27	4.24 \pm 0.25	3.31 \pm 0.31	5.02 \pm 0.22

Note: DBS – day before sprays, DAS – day after spray, Untreated – using water only.

Table 5. Efficacy of the pesticide across survey periods

Sl. No.	Treatments	Effectiveness of the tested pesticide, E (%), Mean \pm SD						
		1 DAS	3 DAS	5 DAS	7 DAS	10 DAS	12 DAS	14 DAS
1	SC product	61.88 \pm 2.27	77.22 \pm 2.91	88.82 \pm 2.46	91.82 \pm 2.05	92.59 \pm 2.89	86.24 \pm 2.61	93.35 \pm 1.73
2	WP product	54.48 \pm 2.31	70.88 \pm 3.05	83.23 \pm 2.79	87.26 \pm 2.11	88.94 \pm 2.39	80.63 \pm 2.86	89.24 \pm 1.96
3	Selecron 500EC	55.64 \pm 2.83	69.00 \pm 3.10	84.38 \pm 2.40	62.74 \pm 4.70	58.19 \pm 3.71	38.51 \pm 4.12	11.90 \pm 2.51
4	Untreated	-	-	-	-	-	-	-

Note: DBS – day before sprays, DAS – day after spray, Untreated – using water only.

decline in the efficacy of Selecron 500 EC after seven days.

By day 14, Selecron 500 EC had lost effectiveness almost completely, with larval density surpassing the threshold of 5 larvae per plant (for maize under 45 days old) at which insecticide intervention is recommended. This can be explained by the effect of high daytime temperatures (reaching up to 40 °C), which likely reduced the insecticidal efficacy and allowed surviving larvae to continue developing. This finding also indicates that encapsulating the active ingredient profenofos in PLA helped reduce the negative impact of light and temperature on the compound. When PLA is used as a carrier for PFF-based pesticides, it not only improves the stability and controlled release of the active ingredient, but also minimises environmental risks. The PLA used in this formulation (Resomer[®] R203H) is specifically designed to fully degrade within three months into CO₂ and water, leaving no harmful residues in soil or water. This ensures safety for both the environment and users. Moreover, the PLA matrix enhances the adhesion and penetration of PFF on plant surfaces, thereby increasing pest control efficiency while maintaining ecological compatibility. In contrast, the SC and WP formulations prepared from PFF/PLA scaffolds sustained their insecticidal efficacy across the full observation period.

As it was presented in Table 5, the SC and WP formulations incorporating PFF/PLA scaffolds maintained high levels of insecticidal efficacy,

reaching 93.35% and 89.24%, respectively, at 14 days after application. In contrast, the conventional formulation Selecron 500 EC showed a steep decline in performance, with efficacy dropping to only 11.9% over the same period. This sharp reduction aligns with the well-documented instability of profenofos under field conditions, where sunlight exposure, elevated temperatures, and microbial activity accelerate degradation. Consistent with earlier reports and manufacturer specifications, profenofos generally demonstrates peak activity within 5–7 days after application, after which its effectiveness decreases rapidly. By day 14, its capacity to suppress *Spodoptera frugiperda* populations is severely diminished.

The extended efficacy observed for the PFF/PLA based formulations can be explained by the controlled-release properties imparted by the PLA encapsulation. Release of the active ingredient follows a non-Fickian transport mechanism, driven by the combined effects of Fickian diffusion and polymer relaxation or swelling. This dual mechanism enables gradual diffusion of profenofos from the fibre core, while the PLA shell functions as a protective barrier against environmental stresses such as UV radiation and heat-induced degradation. Consequently, the active compound is better preserved, resulting in significantly prolonged field efficacy compared to conventional pesticide formulations.

Profenofos is a pesticide with specific toxicity and is subject to regulatory control, so

Table 6. Profenofos residues in corn across survey periods

Sl. No.	Treatments	Profenofos residues, mg/kg			
		1 DAS	7 DAS	14 DAS	At harvest
1	SC product	2.01	1.83	1.32	ND
2	WP product	1.94	1.62	1.15	ND
3	Selecron 500EC	3.60	0.61	0.32	ND

Note: DAS – days after spray, ND – not detected.

determining its residues on the plant after application and before harvest is essential. Profenofos residues on maize leaves at 7 and 14 days after application and again before harvest (120 days after sowing) have been determined. The results are presented in Table 6.

The results in Table 6 show that the residue levels in maize leaves were lower for the SC and WP formulations at 1 day after application. However, the residue levels were higher at 7 and 14 days. After 14 days, the residue levels from the SC and WP formulations were even 3.2 times higher than those from Selecron 500 EC. This outcome suggests that profenofos loses effectiveness under light and heat, while the PLA coating slows this degradation. As a result, more profenofos remains on the leaves, which means the formulation continues to be effective against pests. However, it can also be seen that at harvest, none of the three tested formulations showed detectable residue levels.

The findings of this study highlight the potential benefits of PFF/PLA nanofibres pesticide formulations for sustainable pest management in tropical agricultural systems such as Vietnam. By maintaining insecticidal efficacy for up to two weeks after a single application, these nano formulations can substantially reduce the frequency of pesticide sprays. This not only lowers labour requirements and application costs but also minimises operator exposure to toxic chemicals. Furthermore, the controlled-release mechanism reduces the likelihood of excessive residues in food crops and limits pesticide runoff into surrounding soil and water systems. Such improvements contribute directly to environmental protection, preservation of biodiversity, and alignment with integrated pest management strategies.

These results are also consistent with those obtained by our research group in a previous study using fenobucarb as the active ingredient and tested on rice plants in 2025 (Vu et al., 2025). However, some limitations of this method are evident, particularly the long fabrication time

caused by the low fibre production rate, which affects its feasibility for large-scale applications. To address this problem, further studies are needed to improve the electrospinning setup by designing the device with multiple nozzles (for example, 2, 4, or 6 nozzles), incorporating an electromagnetic field focusing module to concentrate the electric field and reduce fibre loss during electrospinning, and more accurately determining the amount of active ingredient required to suppress pests, thereby optimising pesticide usage. These approaches would indirectly enhance the productivity of the electrospinning device.

Overall, the superior field performance of the SC and WP nano formulations demonstrates their potential as promising alternatives to conventional profenofos products, providing a practical pathway toward more efficient, economical, and environmentally responsible pest control in maize cultivation. However, prolonged exposure may cause neurological or respiratory effects, so proper safety precautions during formulation, handling, and field application are essential. Regulatory agencies, including the WHO and FAO, have established strict limits on its use and residue levels in crops. In this study, the nano-formulated PFF in PLA aimed to reduce direct exposure and control the release rate, which may lower toxicity risks. However, comprehensive residue analysis and ecotoxicological evaluation are still required to confirm the environmental safety of this formulation.

CONCLUSIONS

This study successfully developed core/shell nanofibres incorporating profenofos within a polylactic acid matrix using electrospinning, producing fibres with an average diameter of 495.74 ± 86.46 nm. Release experiments indicated an initial 32.6% release within two weeks and a cumulative 82.15% release over 15 weeks, consistent with a non-Fickian transport mechanism

governed by both diffusion and polymer relaxation. The nanofibers were formulated into suspension concentrate and wettable powder products, which maintained field efficacies of 93.35% and 89.24%, respectively, in maize, compared with only 11.9% for the commercial formulation Selecron 500 EC.

These findings demonstrate the potential of PFF/PLA nanofibres as an effective slow-release pesticide system, offering prolonged efficacy, reduced application frequency, and lower environmental impact. Beyond maize, this approach highlights the promise of nanotechnology in pesticide formulation, contributing to safer, more efficient, and environmentally sustainable crop protection strategies. These findings also indicate the need to conduct additional experiments related to residue measurements as well as to address regulatory implications and ecotoxicity.

Acknowledgments

The authors would like to thank the Functional Polymer Laboratory (SMSE) for providing measurement equipment support for this research, Prof. Vu T.K (School of Chemistry and Life Science- HUST), Mr. Vu V.V (Northern Plant Protection Drug Inspection and Testing Center, Hanoi, Vietnam), and Mr. Tuan T.M (Center for Research and Consulting on the Development of Plant Protection Drugs and Fertilizers) for their assistance in preparing the pesticide and conducting field trials.

REFERENCES

- Ahlawat S., Malik K., Kumari N., Malik K., Arya S., (2021), Nano-enabled pesticides in agriculture: budding opportunities and challenges, *Journal of Nanoscience and Nanotechnology*, 21, 3337–3350. <https://doi.org/10.1166/jnn.2021.19018>
- Akhtar H., Usman M., Binyamin R., Hameed A., Arshad S.F., Aslam H.M.U., Khan I.A., Abbas M., Zaki H.E.M., Ondrasek G., Shahid M.S., (2024), Traditional strategies and cutting-edge technologies used for plant disease management: A comprehensive overview, *Agronomy*, 14(9), 2175. <https://doi.org/10.3390/agronomy14092175>
- An C., Sun C., Li N., Huang B., Jiang J., Shen Y., Wang C., Zhao X., Cui B., Wang C., Li X., Zhan S., Gao F., Zeng Z., Cui, H., Wang, Y., (2022), Nanomaterials and nanotechnology for the delivery of agrochemicals: Strategies towards sustainable agriculture, *Journal of Nanobiotechnology*, 20(11), 2–19. <https://doi.org/10.1186/s12951-021-01214-7>
- Audelo M.L.D.P., Chávez S.A.B., Ruíz, S.C.G., Parra H.H., Kerdan I.G., González J.M.R., Rad J.S., Gómez G.L., (2022), Stability phenomena associated with the development of polymer-based nano pesticides, *Oxidative Medicine and Cellular Longevity*, 2022, 1–15. <https://doi.org/10.1155/2022/5766199>
- Chen C., Zou W., Cui G., Tian J., Wang Y., Ma L., (2020), Ecological risk assessment of current-use pesticides in an aquatic system of Shanghai, China, *Chemosphere*, 257, 127222. <https://doi.org/10.1016/j.chemosphere.2020.127222>
- Crop Protection Chemicals Market Size, Share & Industry Analysis, By Type (Herbicides, Insecticides, Fungicides, and Others), By Source (Synthetic Chemicals and Biologicals), By Mode of Application (Foliar Spray, Soil Treatment, Seed Treatment, and Others), By Crop Type, and Regional Forecast, 2025–2032, (2025). <https://www.fortunebusinessinsights.com/industry-reports/crop-protection-chemicals-market-100080> (Accessed: 31 July 2025)
- Eash L., Fonte S.J., Sonder K., Honsdorf N., Schmidt A., Govaerts B., Verhulst N., (2019), Factors contributing to maize and bean yield gaps in Central America vary with site and agroecological conditions, *The Journal of Agricultural Science*, 157(4), 300–317. <https://doi.org/10.1017/S0021859619000571>
- Ficke A., Cowger C., Bergstrom G., Brodal G., (2018), Understanding yield loss and pathogen biology to improve disease management: Septoria nodorum blotch - A case study in wheat, *Plant Disease*, 102(4), 696–707. <https://doi.org/10.1094/PDIS-09-17-1375-FE>
- Jain H.V., Dhiman S., Ansari N.G., (2024), Recent trends in techniques, process and sustainability of slow-release formulation for pesticides, *Industrial Crops and Products*, 216, 118764. <https://doi.org/10.1016/j.indcrop.2024.118764>
- Jayaraj R., Megha P., Sreedev P., (2016), Organochlorine pesticides, their toxic effects on living organisms and their fate in the environment, *Interdisciplinary Toxicology*, 9(3), 90–100. <https://doi.org/10.1515/intox-2016-0012>
- Khatri N., Tyagi S., (2015), Influences of natural and anthropogenic factors on surface and groundwater quality in rural and urban areas, *Frontiers in Life Science*, 8(1), 23–39. <https://doi.org/10.1080/21553769.2014.933716>
- Leskovac A., Petrović S., (2023), Pesticide use and degradation strategies: Food safety, challenges and perspectives, *Foods*, 12(14), 2709. <https://doi.org/10.3390/foods12142709>
- Modafferi A., Ricupero M., Mostacchio G., Latella

- I., Zappala L., Palmeri V., Garzoli S., Giunti G., Campolo O., (2024), Bioactivity of *Allium sativum* essential oil-based nano-emulsion against *Planococcus citri* and its predator *Cryptolaemus montrouzieri*, *Industrial Crops and Products*, 208, 117837. <https://doi.org/10.1016/j.indcrop.2023.117837>
14. Oerke E.C., (2006), Crop losses to pests, *The Journal of Agricultural Science*, 144(1), 31-43. <https://doi.org/10.1017/S0021859605005708>
15. Ristaino J.B., Anderson P.K., Bebber D.P., Brauman K.A., Cunniffe N.J., Fedoroff N.V., Finegold C., Garrett K.A., Gilligan C.A., Jones C.M., Martin M.D., MacDonald G.K., Neenan P., Records A., Schmale D.G., Tateosian L., Wei Q., (2021), The persistent threat of emerging plant disease pandemics to global food security, *PNAS*, 118(23), 1-9. <https://doi.org/10.1073/pnas.2022239118>
16. Roshani B., Tavanai H., Morshed M., Khajehali J., (2016), Controlled release of thiram pesticide from poly (L-lactic acid) nanofibers, *The Journal of the Textile Institute*, 108(9), 1-6. <https://doi.org/10.1080/00405000.2016.1258950>
17. Schneider K., Hurle J.B., Cerezo E.R., (2023), Pesticide reduction amidst food and feed security concerns in Europe, *Nature Food*, 4, 746-750. <https://doi.org/10.1038/s43016-023-00834-6>
18. Sun Y., Wang S., Li M., Xiong M., Zhang, H., (2025), Construction of hybrid nano catalyst with enhanced enzymatic and photo-Fenton catalytic activity for the efficient detoxification of profenofos, *Journal of Environmental Management*, 384, 125577. <https://doi.org/10.1016/j.jenvman.2025.125577>
19. Sur S., Shathivelu M., (2022), A concise overview on pesticide detection and degradation strategies, *Environmental Pollutants and Bioavailability*, 34(1), 112-126. <https://doi.org/10.1080/26395940.2022.2041489>
20. Vu D. A., Le T.H.A., Tuan A.P., Duc V.M., Vu T.K., Liem T.N (2025), Controlled-release pesticide nanofibers for sustainable agriculture: Effects of processing parameters on fiber morphology and release kinetics, *Journal of Ecological Engineering*, 26(6), 48–61. <https://doi.org/10.12911/22998993/201995>
21. Wagh V., Mukate S., Muley A., Kadam A., Panaskar D., Varade A., (2020), Study of groundwater contamination and drinking suitability in basaltic terrain of Maharashtra, India through PIG and multivariate statistical techniques, *Journal of Water Supply: Research and Technology - AQUA*, 69(4), 398-414. <https://doi.org/10.2166/aqua.2020.108>
22. Wang D., Saleh N.B., Byro A., Zepp R., Demessie E.S., Luxton, T.P., Ho K.T., Burgess R.M., Flury M., White J.C., Su C., (2022), Nano-enabled pesticides for sustainable agriculture and global food security, *Nature Nanotechnology*, 17, 347-360. <https://doi.org/10.1038/s41565-022-01082-8>
23. Yousef H.A., Fahmy H.M., Arafa F.N., Allah M.Y.A., Tawfik Y.M., Halwany K.K.E., Ashmanty B.A.E., Anany F.S.A, Mohamed M.A., Bassily M.E., (2023), Nanotechnology in pest management: Advantages, applications, and challenges, *International Journal of Tropical Insect Science*, 43, 1387-1399. <https://doi.org/10.1007/s42690-023-01053-z>
24. Yu B., Zeng J., Gong L., Zhang M., Zhang L., Chen X., (2007), Investigation of the photocatalytic degradation of organochlorine pesticides on a nano-TiO₂ coated film, *Talanta*, 72(5), 1667-1674. <https://doi.org/10.1016/j.talanta.2007.03.013>
25. Zaitoon A., Lim L.T., Dupree C.S., (2021), Activated release of ethyl formate vapor from its precursor encapsulated in ethyl cellulose/poly (ethylene oxide) electrospun nonwovens intended for active packaging of fresh produce, *Food Hydrocolloids*, 112, 106313. <https://doi.org/10.1016/j.foodhyd.2020.106313>
26. Zhou W., Li M., Achal V., (2025), A comprehensive review on environmental and human health impacts of chemical pesticide usage, *Emerging Contaminants*, 11(1), 100410. <https://doi.org/10.1016/j.emcon.2024.100410>